Transactions of the 13th International Conference on Structural Mechanics in Reactor Technology (SMiRT 13), Escola de Engenharia - Universidade Federal do Rio Grande do Sul, Porto Alegre, Brazil, August 13-18, 1995

F.E. models of steel-laminated rubber bearings for seismic isolation of nuclear facilities

Forni, M.[1], Martelli, A.[1], Dusi, A.[2], Castellano, G.[3]
1) ENEA-ERG-FISS, Bologna, Italy
2) ENEL-CRIS, Milano, Italy
3) University of Ancona, Italy

ABSTRACT: Non-linear finite-element models of high damping rubber bearings have been developed and implemented in the ABAQUS code in the framework of Italian co-operative studies for seismic isolation development. The hyperelastic models used have been based on the results of tests on rubber specimens. The isolators models are being validated through comparisons of numerical results with complete bearing test data. The main features of the analysis are reported, together with an example of validation.

1 INTRODUCTION AND SCOPE

Aim of this study is the implementation, in the ABAQUS code, and validation of non-linear (both axisymmetric and three-dimensional) finite-element models (FEMs) of High Damping steel-laminated Rubber Bearings (HDRBs) used for the seismic isolation of civil structures and industrial plants. The work has been performed in the framework of the Italian activities on seismic isolation development and application (see Marioni et al. 1995 and Forni et al. 1995a). Validation of the models is based on the results of a wide ranging experimental campaign which is in progress at ISMES on single HDRBs (Martelli et al. 1995a).

2 ISOLATORS CONSIDERED

The HDRBs are formed by alternate vulcanized rubber layers and steel plates, bonded together by use of chemical compounds. They are usually placed between the structure and its foundations. Their features provide high stiffness in the vertical direction (to support the dead load) and low stiffness in the transverse direction (which minimizes amplification of ground acceleration, by leading, however, to large horizontal displacements during strong earthquakes). Figure 1 shows the sketch of an optimized full-scale isolator, manufactured by ALGA, which is being analysed in the above-mentioned experimental campaign. Three different *scales* (1:1, 1:2 and 1:4) and two *shape factors* (S = 12 and S = 24) are being considered in the tests for this bearing. This study refers to the half scale isolators with S=12 shape factor, because only for these measured data are already available.

In addition, five *attachment systems* between the isolator and the structure are being considered in the experiments: 'recess', 'bolts', 'bolts & central dowel', 'central dowel' and

'bonding'. 'Recess' and 'central dowel' attachments are very similar and the most difficult to model because they involve monolateral contact between rigid surface and deformable body. 'Bolts', 'bolts & central dowel' and 'bonding' attachment systems are practically equivalent from the kinematic point of view and correspond to a perfect encastre of the two bases of the isolator to the structure. In this work, only the 'recess' and 'bolts' attachments have already been considered (see Figure 2-a, b).

As regards *materials*, because the HDLRBs are characterized by a highly non-linear behaviour in terms of stiffness, a hyperelastic model is necessary for the rubber and an elastic-plastic for steel (at large displacements) to correctly describe the actual behaviour. HDRB damping is pratically independent of velocity and non-linearly dependent on displacement (hysteretic damping). Its effects on the isolator stress distribution and stiffness have been neglected in the present step of the analysis. In a near future, an appropriate model (UMAT subroutine in ABAQUS) will be prepared to take into account the damping behaviour. Although two different rubber compounds (soft, G = 0.4 MPa, and hard, G = 0.8 MPa), developed by MRPRA, have been considered in the tests, the hard rubber only has been analysed to date. This rubber is the most difficult to model, due to the high design loads which involve some creep and plastic effects, impossible to be calculated by the hyperelastic theory.

Finally, as regards *loads*, it is noted that the full-scale isolator of Figure 1 supports a design vertical load of 1600 kN (800 kN in the case of soft rubber). In order to have the actual stress in the rubber (which is required by a correct application of similitude laws), the values for the 1:2 and 1:4 scales have been 400 kN and 100 kN respectively (the half in the case of soft rubber). The design shear strain (that is the shear strain corresponding to design earthquake) has been assumed to be 100% of the total rubber thickness (150 mm for the full scale in the tests of Martelli et al. 1995a). Qualification tests are generally carried out up to twice the design displacement (i.e. generally to at least 200% shear strain) under the design vertical load; during failure tests, 400% shear strain is often exceeded (Martelli et al. 1995a). Figures 3-a and 3-b show a compression and a shear test under vertical compression load on a half-scale isolator performed using SISTEM.

3 FINITE ELEMENT MODELS

Axisymmetric models of the above-mentioned isolators have been developed and implemented in ABAQUS (see ABAQUS User's Manual). Due to the geometry considered and the loads applied (see Figures 2, 3), axisymmetric elements with non-axisymmetric deformation have been used to model the seismic isolator. Some detailed meshes have been analysed in order to reach stability and convergence. A minimum of three layers of CAXA4Hn elements for each rubber layer have been necessary to model the rubber parts (n=1 is generally sufficient). SAXA11 shell elements have been used for the steel plates. Seven subdivisions along the radius have been sufficient for the 'bolts' attachment systems, thus the isolator FEM consists of 630 CAXA4H1 elements and 224 SAXA11 shell elements in the case of the lower shape factor and 1260 CAXA4H1 elements and 434 SAXA4H1 shell elements in that of the higher shape factor.

In addition to axisymmetric models, a *three-dimensional model* has been implemented to verify the CAXA elements' behaviour, to model the monolateral 'recess' attachment system and to reach large non-axisymmetric shear strains. 3D models are also usefull to correctly describe the tensile stress on bolts (if present), combined compression - shear - torsion stress-strain distribution (if eccentricity is relevant), presence of defects, and effects of the construction tolerances and others asymmetries. Some 3D meshes have

been implemented using PREABC, a computer program developed by ENEA which writes the ABAQUS input files for 3D cylindrical models based on a few geometric input data. In this case also, 7 subdivision along the radius and three layers of solid (C3D8H) elements for each rubber layer have been necessary to model the rubber. Steel plates have been modelled by using S4R5 shell elements. Taking into account 32 subdivision along the external circumference, the 3D model for the lower shape factor isolator includes 9680 nodes and 4868 elements and requires a minimum of four hours of CPU time on a RISC6000 work station (against ten minutes of the axisymmetric model) for the execution of two static steps (compression and shear).

4 HYPERELASTIC MODEL

The hyperelastic model of ABAQUS is based on the definition of the stress components as function of the strain energy potential U, a very complex function of λ_i (principal stretch ratio, which is the current specimen length over the original length in the principal i-direction), $C_{i,j}$ (material constants describing the hyperelastic behaviour) and D_i (material constants describing compressibility, equal to zero for incompressible materials). The function U is written in polynomial form of the first order (used for small strains) or second order (recommended for large strains). The calibration of the hyperelastic model consists of the definition of the $C_{i,j}$ and (if compressibility is relevant) D_i material constants. This can be done in particular test configurations where, due to the specimen shape and the loading conditions, one or two λ_i components can be neglected or correlated between themselves and some σ_{ij} (stress) components can be put equal to zero, thus considerably simplifying the expression of U.

According to Rebelo (1991) and ABAQUS User's Manual, uniaxial, biaxial and shear experiments on specimens were designed and performed (Martelli et al. 1995a). Each test was performed on 3 specimens drawn from the centre of each rubber batch used for the manufacturing of isolators, both in the unscragged and scragged conditions. It is noted that no compressibility tests were executed, due to the relatively low shape factor of the analysed isolators.

Uniaxial tensile and compression tests must satisfy the following conditions:

$$\sigma_{22} = \sigma_{33} = \sigma_{12} = \sigma_{13} = \sigma_{23} = 0 \qquad (1)$$

$$\lambda_2 = \lambda_3 = 1/\sqrt{\lambda_1} \qquad (2)$$

The correlation (2) is strictly valid for incompressible materials only, which is the case of rubber specimens that have the possibility to strain in two principal directions at least.

The tensile tests were carried out according to ASTM D 412 on dog-bone specimens (30mm x 6mm x 2mm). No significative scattering of test results was detected. Some simple calculations were executed on a single C3D8H element to evaluate the differences of the two hyperelastic models proposed by the ABAQUS User's Manual (Ogden and the above mentioned polynomial). Figure 4 shows the good agreement between both the models and with the measured curve.

The compression tests were carried out according to ASTM D 395 on 3 cylindrical specimens (diameter = 29 mm, height =13 mm) with lubricated bases. In this case also, no significant scattering of test results was present and perfect agreement between the calculated and measured results was found (Figure 5).

As an alternative option to the uniaxial compression tests, *equibiaxial (no shear) tests* may be performed. We executed such tests on thin square specimens (300mm x 300mm x 5mm), strained in the principal directions 1 and 2 (using a constant velocity of 100 mm/min), thus to satisfy the following conditions:

$$\sigma_{11} = \sigma_{22};\ \sigma_{33} = \sigma_{12} = \sigma_{13} = \sigma_{23} = 0 \tag{3}$$

$$\lambda_1 = \lambda_2 = 1/\sqrt{\lambda_3} \tag{4}$$

These tests are quite expensive and rather difficult to be executed, but allow larger deformations to be achieved with respect to the compression tests, where friction between the specimen and the test device does not permit to reach strains higher than 35% in real uniaxial conditions (see equations 1 and 2). Figure 6 shows the equipment that we used for the equibiaxial tests and the optical instrumentation that we adopted to measure the strain in the central part of the specimen, far away from boundary perturbations. The calculated and measured stress-strain curves don't agree perfectly in this case (Figure 7); however, for the second order polynomial model, the agreement can be considered sufficient.

Finally, *planar (pure shear) tests* were carried out on rectangular specimens (300mm x 120mm x 5mm) strained along their longer edge (principal direction=1), using a constant velocity of 100 mm/min, in order to satisfy the following condions:

$$\sigma_{33} = 0 \tag{5}$$

$$\lambda_2 = 1;\ \lambda_1 = 1/\lambda_3 \tag{6}$$

The test equipment shown in Figure 8 allowed for large displacements; in fact, the optical instrumentations measured a strain larger than 300% in the central part of the specimens. In this case also, the second order polynomial model provided the best agreement with the experimental results (Figure 9).

5 VERIFICATION OF THE ISOLATOR FEMs

Based on the results of the previous section, the polynomial hyperelastic model with N=2 has been adopted for the analysis of the experimental tests on the complete isolators. The curves shown in Figures 4, 7 and 9 were used for input data.

An axisymmetric model with five elements for each rubber layer was used for calculating the *vertical stiffness*. Both scragged and unscragged rubber hyperelastic models with input data at 150% for uniaxial test, 120% for biaxial test and 300% for planar test, were used. Figure 10 shows that the agreement between the calculated and measure values for the unscragged rubber is good up to the design load (400 kN), then the model becames too stiff. This is probably due to rubber plasticity and creep phenomena occurred during the isolator tests at high loads. For the scragged rubber, the agreement is good to 1.5 times the design vertical load.

Both axisymmetric (for low shear strains) and 3D models (for high shear strains) were used for calculating the *horizontal stiffness* at 50%, 100% and 200% shear strain, under the design vertical compression load (Martelli et al. 1995a). Due to the quite large range of deformation, it is not possible to use a unique hyperelastic model, but an appropriate

model must be calibrated for each deformations of interest. For the evaluation of the horizontal stiffness at 50% shear strain, an axisymmetric FEM (with three layers of elements for each rubber layer) using the unscragged rubber input data not exceeding 100% for uniaxial and biaxial tests and 150% for planar test, had to be used. Figure 11 shows that the agreement between the calculated and measured horizontal stiffness is very good, taking into account that the model has no damping (thus the hysteresis loop connot be reproduced). For the evaluation of the horizontal stiffness at 100% shear strain, the same model for the unscragged rubber, including uniaxial input data up to 150%, biaxial input data up to 120% and planar input data up to 300%, had to be used. In this case also, the agreement between the calculated and measured values was good (see Figure 12), but the unscragged model became too rigid at high deformations, with respect to the isolator, which was subjected to the two cycles at 50% shear strain. For higher shear strains, a 3D FEM and a scragged rubber model (with input data for the hyperelastic model mostly concentrated at large strains) had to be used. We found a good agreement between calculated and measured values to 180% shear strain, then the model became too stiff (partly due to some inaccurancy of the hyperelastic model related to insufficient conditioning of specimens), similar to the case of the vertical stiffness calculation. Anyway, it has been confirmed that the hyperelastic model can be used at large shear strains to analyse the stress distribution (Figure 13) and identify the most stressed parts of the isolator. To this aim, some parametric calculations have been performed in order to evaluate the effects of the attachment system, shape factor, steel plate thickness, central hole diameter, etc., on the rubber stress. The first results of this analysis (which is still in progress) show that the 'recess' attachment system is less stiff than the 'bolted' system (which is in agreement with the experimental results) and that the central hole significantly decreases the stress on the rubber, but increases that in the steel plates. More details will be reported by Forni et al. (1995a & b).

CONCLUSIONS AND FUTURE WORK

This paper has summarized the main features of numerical activities which are in progress for the development and validation of finite-element models of steel-laminated high damping rubber bearings. An example of validation has been presented. Such a work will be completed by including damping models and will be extended to all the isolators considered in the tests of Martelli et al. (1995a), namely to optimized isolators with different sizes, rubber compounds, attachment systems, and shape factors. Updated results will be presented by Forni et al. (1995a & b).

The availability of reliable isolators' models will allow the number of quite costly experimental tests on complete bearings to be considerably limited, not only as regards the analysis of the effects of some important parameters (e.g. temperature, ageing, vertical load on horizontal stiffness, etc.), but also for complicated experiments like for instance, failure tests and analysis of the effects of defects.

Should the models developed be sufficiently reliable, they may be used for bearing qualification, as stressed by Martelli et al. (1995b).

Finally, as soon as the experiments of Martelli et al. (1995a) on structure mock-ups isolated by means of the bearings under consideration will be completed, numerical analysis will also be performed to analyse these tests.

REFERENCES

ABAQUS User's Manual - Version 5.3. Pawtucket: Hibbit, Karlsson & Sorensen, Inc.

Forni, M. & A. Martelli 1995a. Finite-element models of rubber bearings and guidelines development for isolated nuclear facilities in Italy. *Proc. Post-SMiRT Conf. Seminar on Seismic Isolation, Passive Energy Dissipation and Active Control of Structures, Santiago, 21-23 August 1995.*

Forni, M., Martelli, A., Dusi, A. and G. Castellano 1995b. Hyperelastic models of steel-laminated rubber bearings for the seismic isolation of civil buildings and industrial plants. *Proc. ABAQUS User's Conf., Paris, 31 May - 2 June 1995.*

Marioni, A., Martelli, A., Forni, M., Bonacina, G., Bettinali, F. & C. Mazzieri 1995. Progress in applications and experimental studies for isolated structures in Italy. *Proc. Post-SMiRT Conf. Seminar on Seismic Isolation, Passive Energy Dissipation and Active Control of Structures, Santiago, 21-23 August 1995.*

Martelli, A., Forni, M., Spadoni, B., Marioni, A., Bonacina, G. & G. Pucci 1995a. Progress of Italian experimental activities on seismic isolation. *Proc. 13th Int. SMiRT Conf., Porto Alegre, 13-18 August 1995.* Rotterdam: Balkema.

Martelli, A., Forni, M., Bergamo, G., Bonacina, G., Cesari, G.F., Di Pasquale, G. & M. Olivieri 1995b. Proposal for design guidelines for isolated nuclear reactors. *Proc. Post-SMiRT Conf. Seminar on Seismic Isolation, Passive Energy Dissipation and Active Control of Structures, Santiago, 21-23 August 1995.*

Rebelo, N. 1991. Analysis of rubber components with ABAQUS. *Proc. of 2° National Congress of ABAQUS Users' Group Italia, Bologna, Italy, March 21-22.*

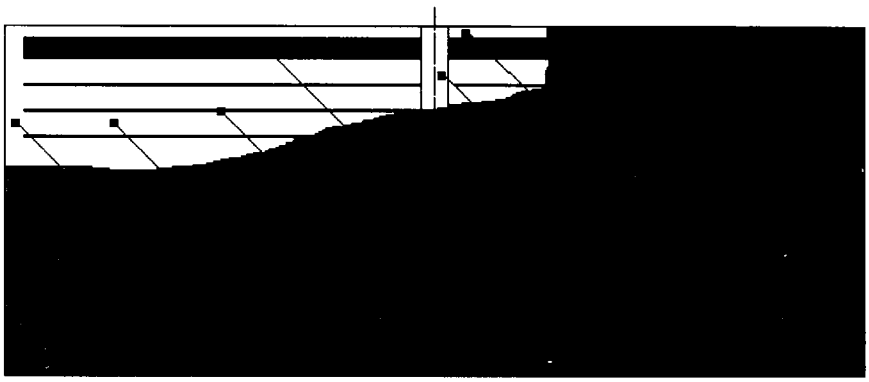

Figure 1. Sketch of the full-scale HDRB

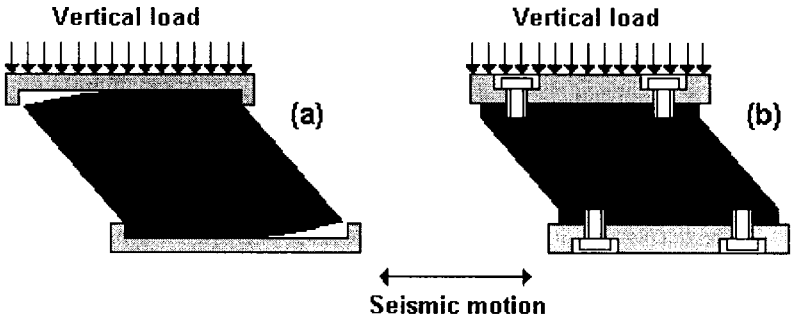

Figure 2. 'Recess' (a) and 'bolts' (b) attachment systems.

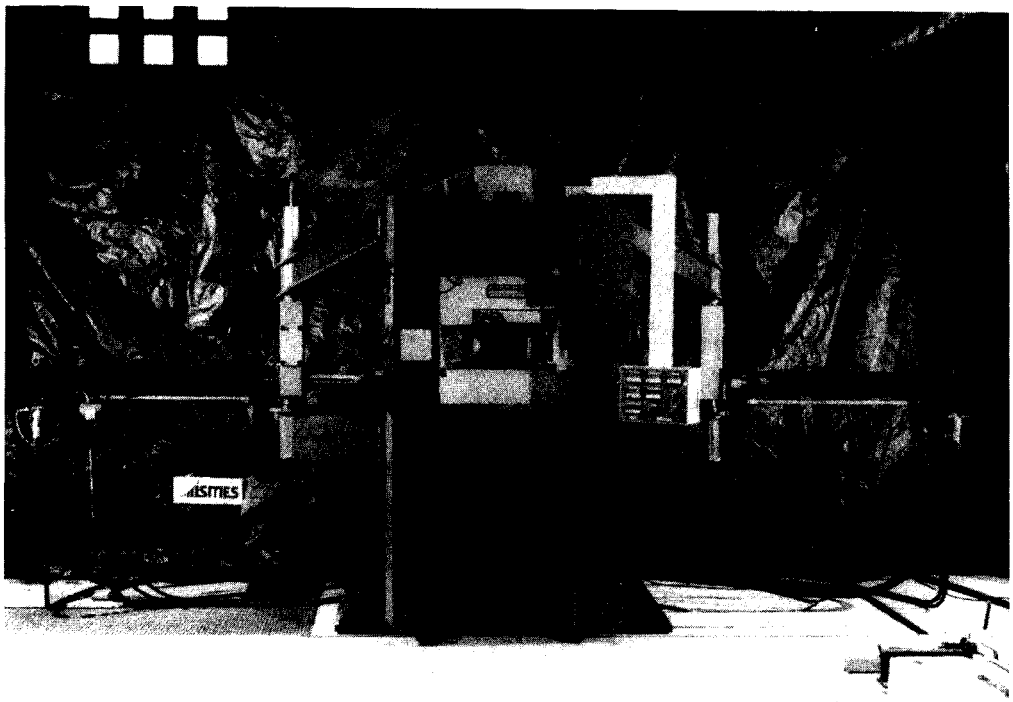

Figure 3a. Compression test performed on SISTEM on HDRB.

Figure 3b. Combined compression & shear test performed on SISTEM on HDRB.

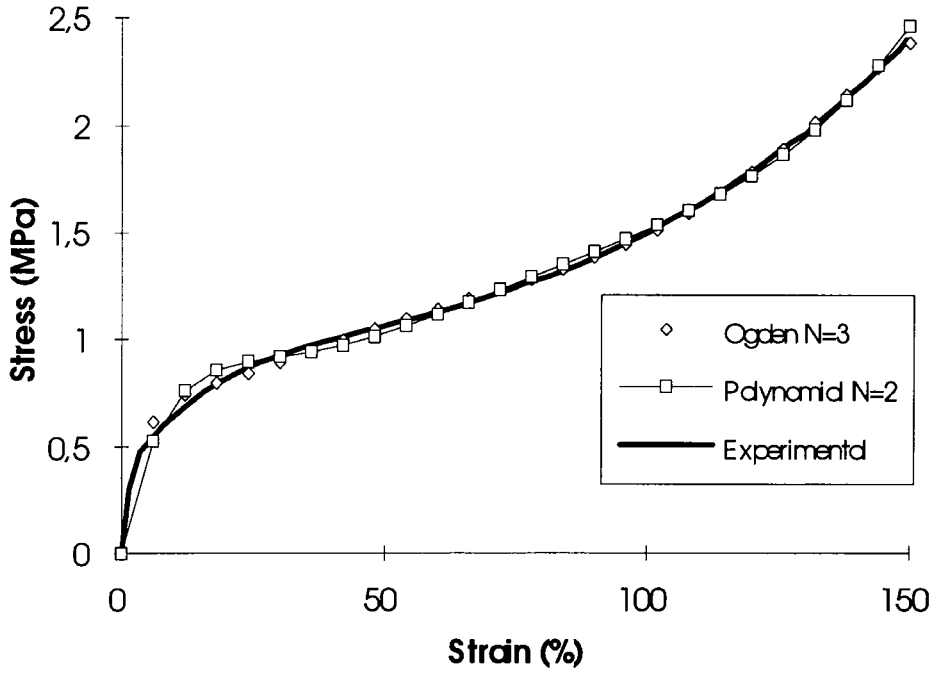

Figure 4. Comparison between measured and calculated stress-strain values for a tensile test on unscragged rubber compound

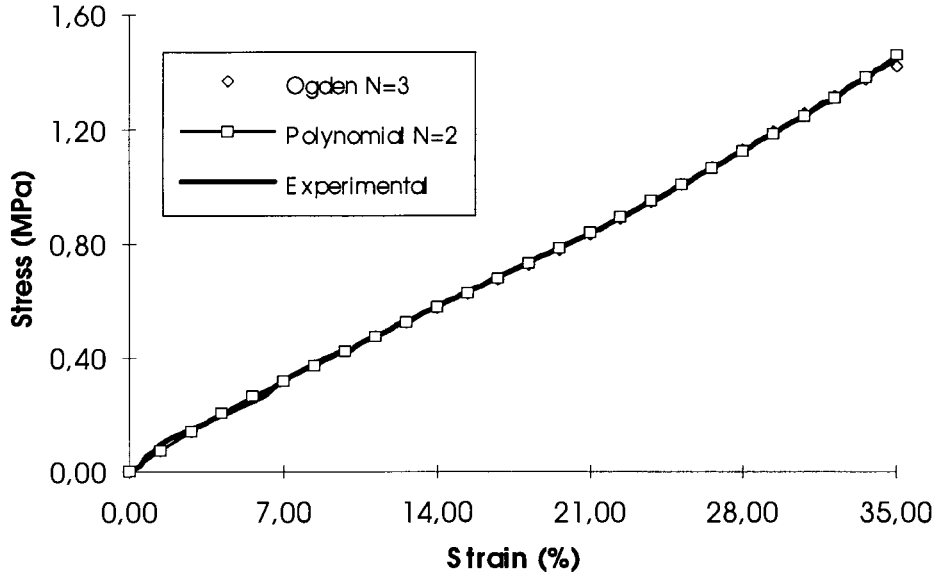

Figure 5. Comparison between measured and calculated stress-strain values for a compression test on unscragged rubber compound

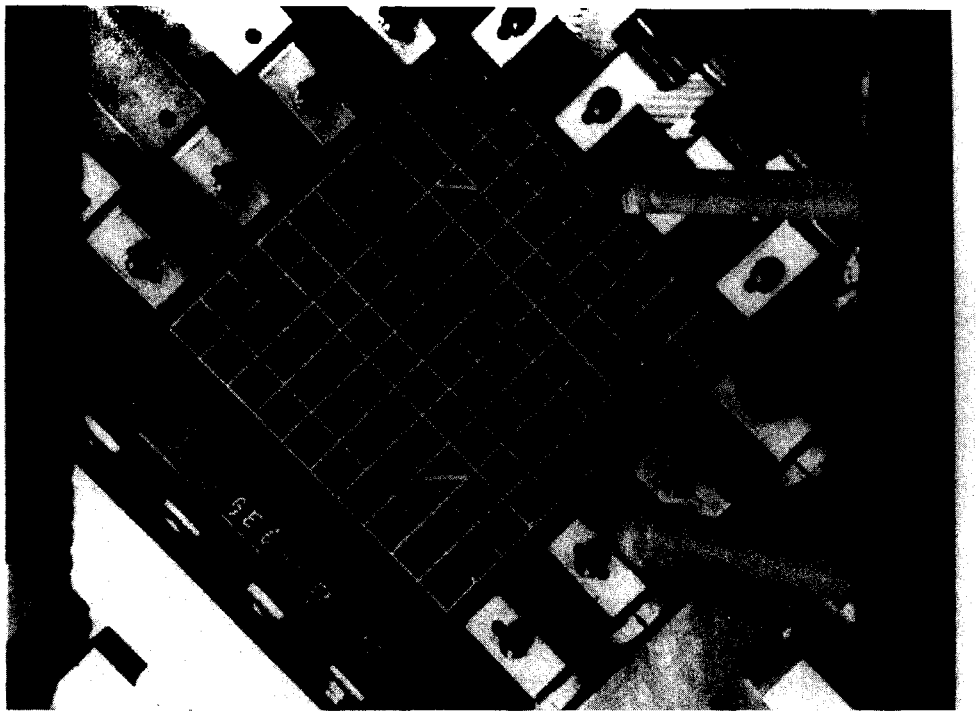

Figure 6. Execution of an equibiaxial (no shear) test

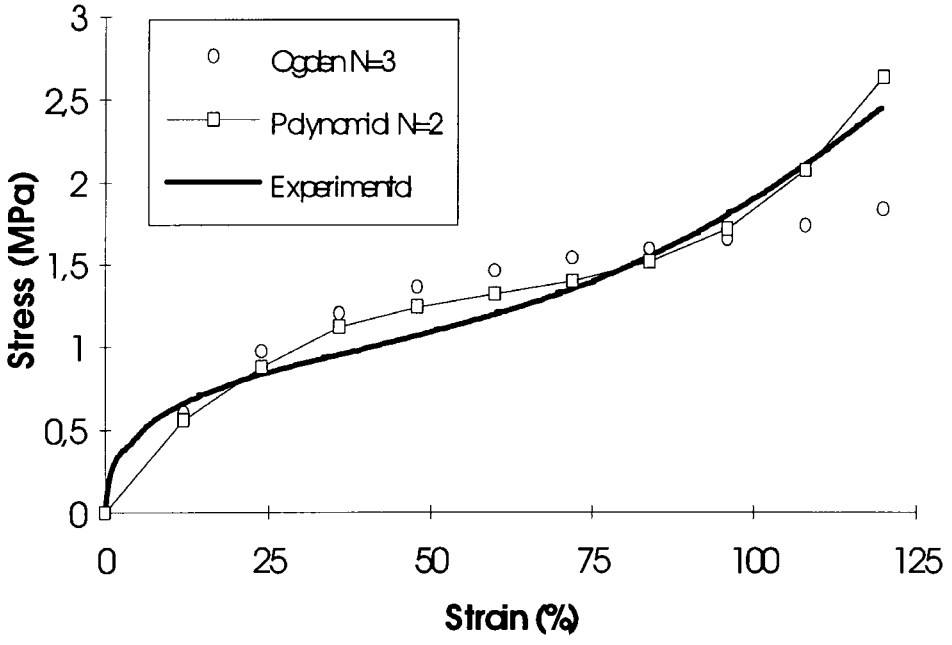

Figure 7. Comparison between measured and calculated stress-strain curves for an equibiaxial test on unscragged hard rubber compound

Figure 8. Execution of a planar (pure shear) test

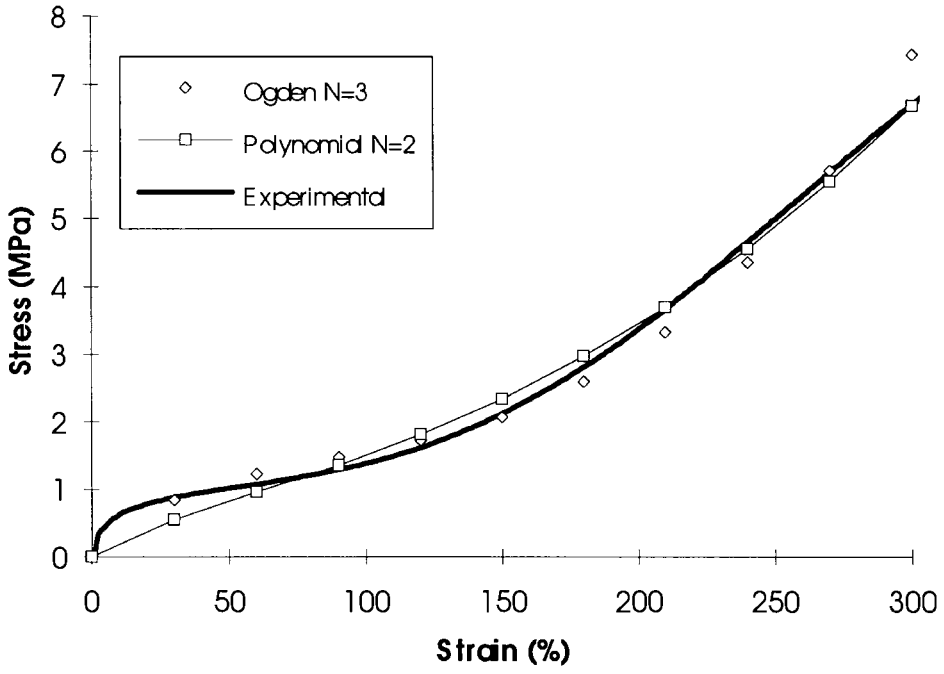

Figure 9. Comparison between measured and calculated stress-strain curves for a planar test on unscragged hard rubber compound

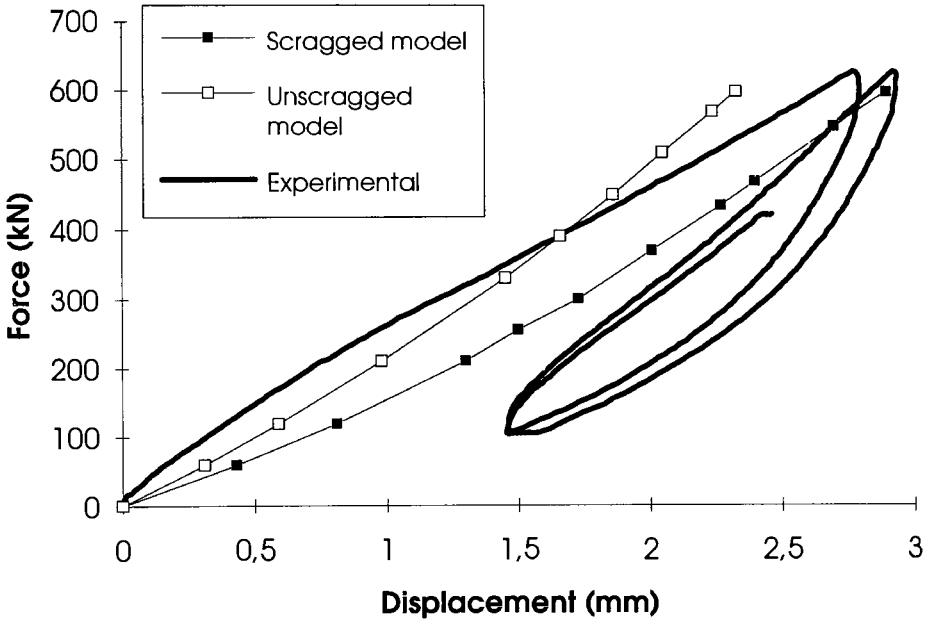

Figure 10. Comparison between measured and calculated force-displacement values for a compression test at 150% design vertical load of a complete bearing

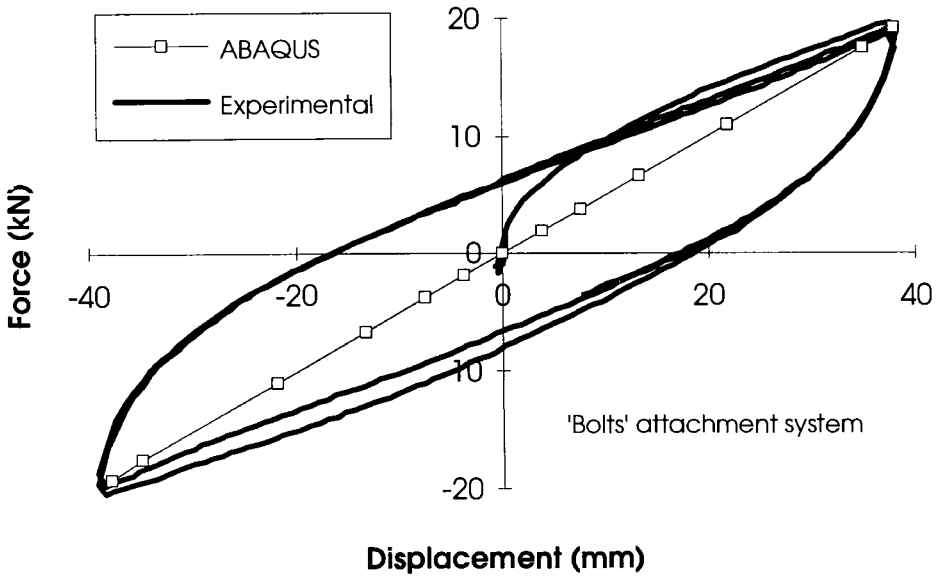

Figure 11. Comparison between measured and calculated force-displacement values for a combined compression & 50% shear strain test of a complete bearing

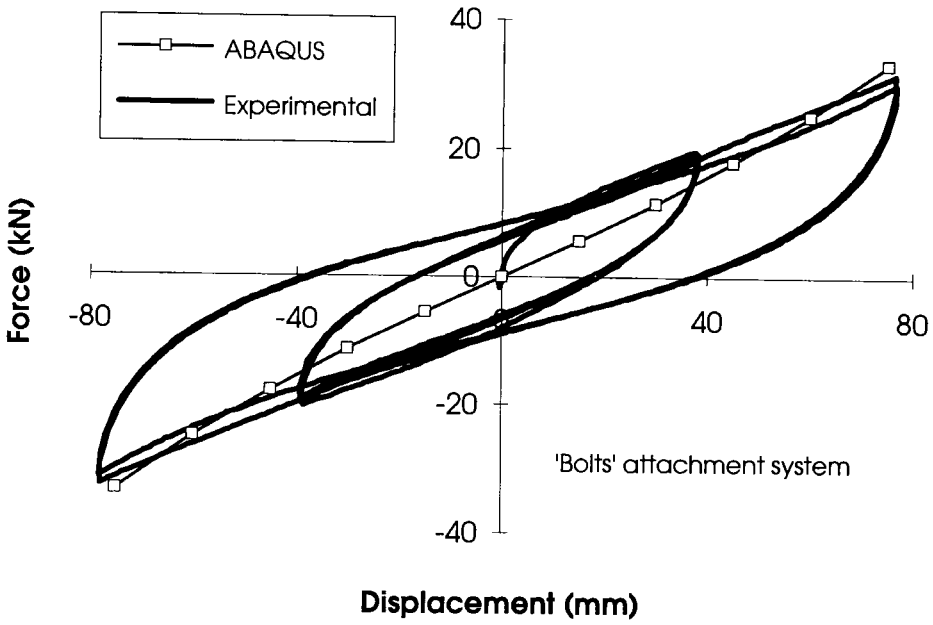

Figure 12. Comparison between measured and calculated force-displacement values for a combined compression & 100% shear strain test of a complete bearing

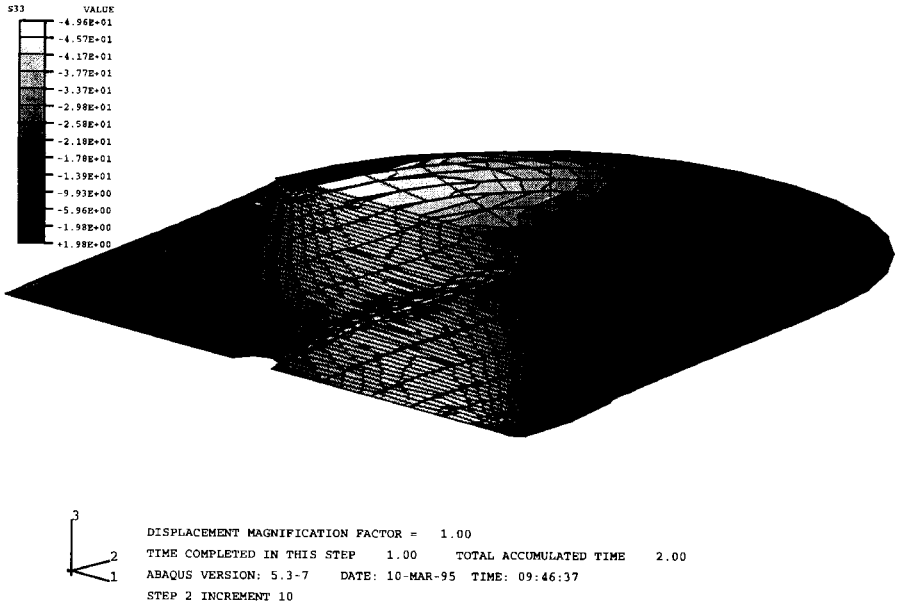

Figure 13. Stress distribution in the 3D model of the 'bolted' isolator at 200% shear strain under the design vertical load